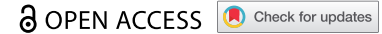Taylor & Francis
Taylor & Francis Group

RESEARCH PAPER

Genetic diversification of persistent *Mycobacterium abscessus* within cystic fibrosis patients

Astrid Lewin ⓘ[a], Elisabeth Kamal[a], Torsten Semmler[b], Katja Winter[c], Sandra Kaiser[c], Hubert Schäfer[a], Lei Mao[a,d], Patience Eschenhagen[e,f], Claudia Grehn[g], Jennifer Bender[h,i], and Carsten Schwarz ⓘ[e,f]

[a]Unit 16 Mycotic and Parasitic Agents and Mycobacteria, Robert Koch Institute, Berlin, Germany; [b]Unit NG 1 Microbial Genomics, Robert Koch Institute, Berlin, Germany; [c]Unit MF1 Bioinformatics, Robert Koch Institute, Berlin, Germany; [d]Unit 31 Infectious Disease Data Science Unit, Robert Koch Institute, Berlin, Germany; [e]Klinikum Westbrandenburg, Campus Potsdam, Cystic Fibrosis Section, Potsdam, Germany; [f]Pediatric Respiratory Medicine, Immunology and Intensive Care Medicine, Charité Universitätsmedizin Berlin, Corporate Member of Freie Universität Berlin and Humboldt-Universität zu Berlin, Berlin, Germany; [g]Department of Pediatrics, Division of Pulmonology, Immunology and Intensive Care Medicine, Division of Cystic Fibrosis, Charité – Universitätsmedizin, Berlin, Germany; [h]Unit 13 Nosocomial Pathogens and Antibiotic Resistances, Robert Koch Institute, Wernigerode, Germany; [i]ECDC Fellowship Programme, Public Health Microbiology Path (EUPHEM), European Centre for Disease Prevention and Control (ECDC), Solna, Sweden

ABSTRACT

Mycobacterium (*M.*) *abscessus* infections in Cystic Fibrosis (CF) patients cause a deterioration of lung function. Treatment of these multidrug-resistant pathogens is associated with severe side-effects, while frequently unsuccessful. Insight on *M. abscessus* genomic evolvement during chronic lung infection would be beneficial for improving treatment strategies. A longitudinal study enrolling 42 CF patients was performed at a CF center in Berlin, Germany, to elaborate phylogeny and genomic diversification of in-patient *M. abscessus*. Eleven of the 42 CF patients were infected with *M. abscessus*. Five of these 11 patients were infected with global human-transmissible *M. abscessus* cluster strains. Phylogenetic analysis of 88 genomes from isolates of the 11 patients excluded occurrence of *M. abscessus* transmission among members of the study group. Genome sequencing and variant analysis of 30 isolates from 11 serial respiratory samples collected over 4.5 years from a chronically infected patient demonstrated accumulation of gene mutations. In total, 53 genes exhibiting non-synonymous variations were identified. Enrichment analysis emphasized genes involved in synthesis of glycopeptidolipids, genes from the *embABC* (arabino-syltransferase) operon, *betA* (glucose-methanol-choline oxidoreductase) and *cho*D (cholesterol oxidase). Genetic diversity evolved in a variety of virulence- and resistance-associated genes. The strategy of *M. abscessus* populations in chronic lung infection is not clonal expansion of dominant variants, but to sustain simultaneously a wide range of genetic variants facilitating adaptation of the population to changing living conditions in the lung. Genomic diversification during chronic infection requires increased attention when new control strategies against *M. abscessus* infections are explored.

Introduction

More than 30 species of nontuberculous mycobacteria (NTM) are known to cause infections in humans [1], mostly in persons with immunodeficiency or underlying diseases such as Cystic Fibrosis (CF) [2]. NTM prevalence in CF populations is increasing [3], which can in part be attributed to medical progress resulting in extended life expectancy of CF patients. Particularly, infections with *Mycobacterium abscessus* (MABS), also named *Mycobacteroides abscessus*, pose a threat to CF patients as they frequently lead to lung function decrease [4] and pose a risk in lung transplantation [5]. The environment has generally been assumed to be the source of NTM infection.

However, recent findings show that the majority of MABS in CF patients belong to three phylogenetic clusters [6] suggesting human-to-human transmission as an additional potential infection route. MABS is characterized by its extreme resistance toward antibiotics [7], which necessitates long-lasting combination therapy. Despite such protracted therapy causing severe side effects, low culture conversion rates of typically 40–50% have been reported [8]. Because of the serious side effects of the antibiotic therapies, the balance between their harm and benefit for patients must be carefully weighed. Although information on genomic diversity of MABS is now available [6], prognostic genomic markers for disease progression have

not yet been identified. A study by Shaw et al. (2019) has described the genetic diversity of MABS isolated from different body sites of two CF patients shortly (up to 59 days) after lung transplantation [9]. Very recently, Bryant et al. (2021) investigated MABS evolution and proposed a model for pathogenic evolution of MABS [10]. Apart from these studies, knowledge on in-patient evolution of MABS during chronicity is still scarce. Using respiratory samples from CF patients from a German CF treatment center, the focus of the present study lies on characterizing the population structure of MABS in CF patients and analyzing genetic variation of MABS evolving within patients during long-term chronic infection.

Materials and methods

Isolation and identification of NTM from Cystic Fibrosis patients

The 42 patients involved in the study were recruited from the CF Center at the Charité-Universitätsmedizin Berlin in Germany from 2013 to 2018. Within this period, the center treated 16 CF patients with NTM-PD. Patient characteristics are summarized in Supplementary Table S1. Respiratory samples (sputum, BAL) were taken in the CF Center, if a patient had an unclear decline in pulmonary function tests that did not respond to bacteria-targeted antibiotics or during the annual checkup. NTM were isolated from these samples by the Robert Koch Institute. Permission for the study was obtained from the ethics committee of the Charité – Universitätsmedizin Berlin (EA2/093/12). Written consent had been obtained from all patients.

Isolation of NTM from sputum or BAL using Nalc/NaOH was performed as described in [11]. NTM colonies isolated from respiratory samples were purified at least twice by spreading single colonies on agar plates. NTM species were determined by PCR (DreamTaq DNA Polymerase, Thermo Fisher Scientific) and sequencing (ABI BigDyeTM 3.1, Thermo Fisher Scientific) of 16S rDNA and/or ITS. Primers used are listed in Supplementary Table S2.

Cultivation of MABS

MABS was grown at 37°C on Middlebrook 7H11 agar (BD Biosciences) supplemented with 10% modified ADC (2% glucose, 5% BSA, 0·85% NaCl) or in Middlebrook 7H9broth (BD Biosciences) supplemented with 10% modified ADC along with 0.05% Tween 80 without shaking.

Determination of MIC

Minimal inhibitory concentrations (MIC) were determined using the Sensititre™ plates (TREK Diagnostic Systems, ThermoFisher Scientific) according to the instructions of the provider. Interpretation of MIC values followed the CLSI guidelines [12], M62.

Whole genome sequencing

For Illumina sequencing, paired-end DNA libraries were constructed using the Nextera XT DNA kit (Illumina, San Diego, CA, USA) according to the manufacturer´s protocol. The pooled library was prepared as recommended by the Illumina HiSeq v3 reagent preparation guide and loaded onto a cartridge (V3 chemistry) generating a 300 bp paired-end output. MinION one-dimensional (1D) libraries were constructed, using the SQK-RBK004 kit (Nanopore technologies, Oxford, UK), and loaded according to the manufacturer's instructions onto an R9.4 flow cell. The sequencing data was collected for 48 h.

Bioinformatic analysis

NGS data from all 88 MABS isolates from the 11 patients were used for phylogenetic analysis. Reference genomes were *M. abscessus abscessus* (MABSa) ATCC 19977 (NC010397.1), *M. abscessus bolletii* (MABSb) CIP 108541 (NZ_JRMF00000000) and *M. abscessus massiliense* (MABSm) FLAC 047 (NZ_CP021122.1). Identification of global MABS cluster strains was achieved by including one strain of each cluster in the phylogenetic trees [BIR 948, RVI 21, and BIR 1034 (ENA project accession ERP001039) [6]. For quality control of NGS data, the in-house pipeline QCumber (v2.1.1) (https://gitlab.com/RKIBioinformaticsPipelines/QCumber) was used. QCumber employs the software tool Trimmomatic [13], which was used for Illumina adapter removal.

All draft genomes were annotated using Prokka [14]. The determination of the maximum common genome (MCG) alignment was done by identifying the genes present in all genomes [15]. Coding sequences were clustered based on the parameters sequence similarity (min. 70%) and coverage (min. 90%) and defined the 2,085 genes that were present in each genome while fulfilling the threshold parameters as MCG. Next the allelic variants of these genes were extracted from all genomes by a BLAST-based approach, aligned individually for each gene and then concatenated, which resulted in an alignment of 2.089 Mbp. This alignment was used to calculate a maximum likelihood-based

phylogeny with RAxML v.8.2.10 with 100 bootstraps under the assumption of the gtr-gamma DNA substitution model [16]. ClonalFrameML v1.11 [17] was used to correct for recombination events. The phylogenetic tree was visualized together with the distribution of accessory genes using phandango [18].

Interpretation of SNP distances with respect to probability of patient-to-patient transmission was done according to the proposition from Bryant et al., who had proposed less than 20 SNPs to indicate probable recent transmission of MABS, 20–38 SNPs possible recent transmission and more than 38 SNPs no recent transmission [6]. Further confirmation was obtained by comparing the accessory genomes of the isolates.

For gene variation analysis, the genome sequences of 30 MABSa isolates from one chronically infected patient collected in the years 2013 to 2017 were used to extract non-synonymous small nucleotide variants (nsSNV). The MinION sequence data together with Illumina data from an isolate originating from the first sample from this patient were used as a reference to identify nsSNVs in all other isolates compared to this genome sequence. To this end the MinION fast5 output files were demultiplexed with Deepbinner (v.0.2.0) [19]. Basecalling and barcode trimming was performed using Guppy (v.3.1.5) (Community.nanoporetech.com). The read quality was checked using pycoQC (v.2.3.1.2) [20], followed by (1) de-novo assembly of the initial sample, (2) reordering contigs against MABSa ATCC 19977 reference sequence, (3) mapping of the remaining samples from this patient against the final assembly, (4) gene annotation, (5) multi sample variant calling using the initial sample as starting point, (6) SNV and Indel filtering and (7) variant annotation. The assembly was performed using Unicycler (v0.4.7) [21] and reordered with progressiveMauve (v2.4.0) [22] against the MABSa reference sequence. Afterward the remaining samples of the patient were mapped against the assembly using BWA (v0.7.15-r1140). Genes were annotated using prokka (v1.13.3). A multi sample variant calling was performed using GATK (v.4.1.2.0). SNVs and Indels were filtered according to GATKs best practice recommendations with few alterations. For SNVs the following filter was set: QD<2.0 || FS>60.0 || ReadPosRankSum<-8.0 || MQ<40.0 || MQRankSum<-12.5 and for indels QD<2.0 || FS>200.0 || ReadPosRankSum<-20.0. Variants that passed the filter were annotated with SnpEff (v4.3 u) [23]. In a second filtering step only variants in coding regions were selected that cause non-synonymous changes ((countHom() < 30) & (DP ≥ 10) & ((EFF[0].IMPACT = "HIGH") | (EFF[0]. IMPACT = "MODERATE")). Sequence analysis was supported by use of Geneious software (Geneious Prime 2020, Biomatters).

Results

Predominance of MABS among isolated NTM

NTM were isolated from 16 of the 42 patients (Supplementary Table S1). MABS was the most frequently isolated NTM species (11 patients) followed by *M. avium hominissuis* (MAH) (six patients), *M. intracellulare* (three patients) and *M. chimaera* (one patient). Two patients were co-infected by MABS and MAH, one patient by MABS and *M. intracellulare*, one patient by MAH and *M. intracellulare* and one patient by MABS, MAH and *M. intracellulare*.

88 isolates from the 11 patients infected with MABS were further investigated. Seven of these patients were infected with the subspecies MABSa, three with the subspecies MABSm and one patient with the subspecies MABSb. One patient had a double infection with MABSa and MABSb. 43 isolates had a rough, 43 a smooth colony morphology and two were mixed. An overview on isolates used for whole genome sequencing including subspecies, colony morphology, isolation year and accession numbers is presented in Supplementary Table S3.

Absence of patient-to-patient transmission of MABS

Illumina NGS data were used for phylogenetic analysis of all 88 isolates from 34 respiratory samples of 11 MABS-infected patients (Supplementary Table S3). Figure 1 shows a Maximum Likelihood Tree corrected for recombination events based on 2085 core genome genes identified in the genomes of the 88 isolates and the reference strains.

The principle tree structure was confirmed by a Maximum Likelihood Tree based on the pan genome (Supplementary Figure S1).

The phylogenetic tree shows the presence of well-separated MABS clusters each belonging to one patient (A, B, C, H, K, S) as well as the presence of highly similar isolates belonging to different patients (E, F and D, G, O). One representative of each global MABS cluster [6] was included in the phylogenetic tree. While none of the patient isolates formed a cluster with the MABSm global cluster strain BIR 948, isolates from patients E and F clustered with the global MABSa cluster strain RVI 21, whereas isolates D, G and O clustered with global cluster strain BIR 1034. Within MABSa strains up to 32 SNPs between different isolates belonging to one patient were observed in the core genome. Isolates belonging to different MABSa strains within the same global cluster exhibited SNP distances of at least 91 SNPs (cluster D/G/O/BIR 1034) or at least 78 SNPs (cluster E/F/RVI 21), which according to a proposition from Bryant et al. [6] argues against transmission of MABS among patients of the
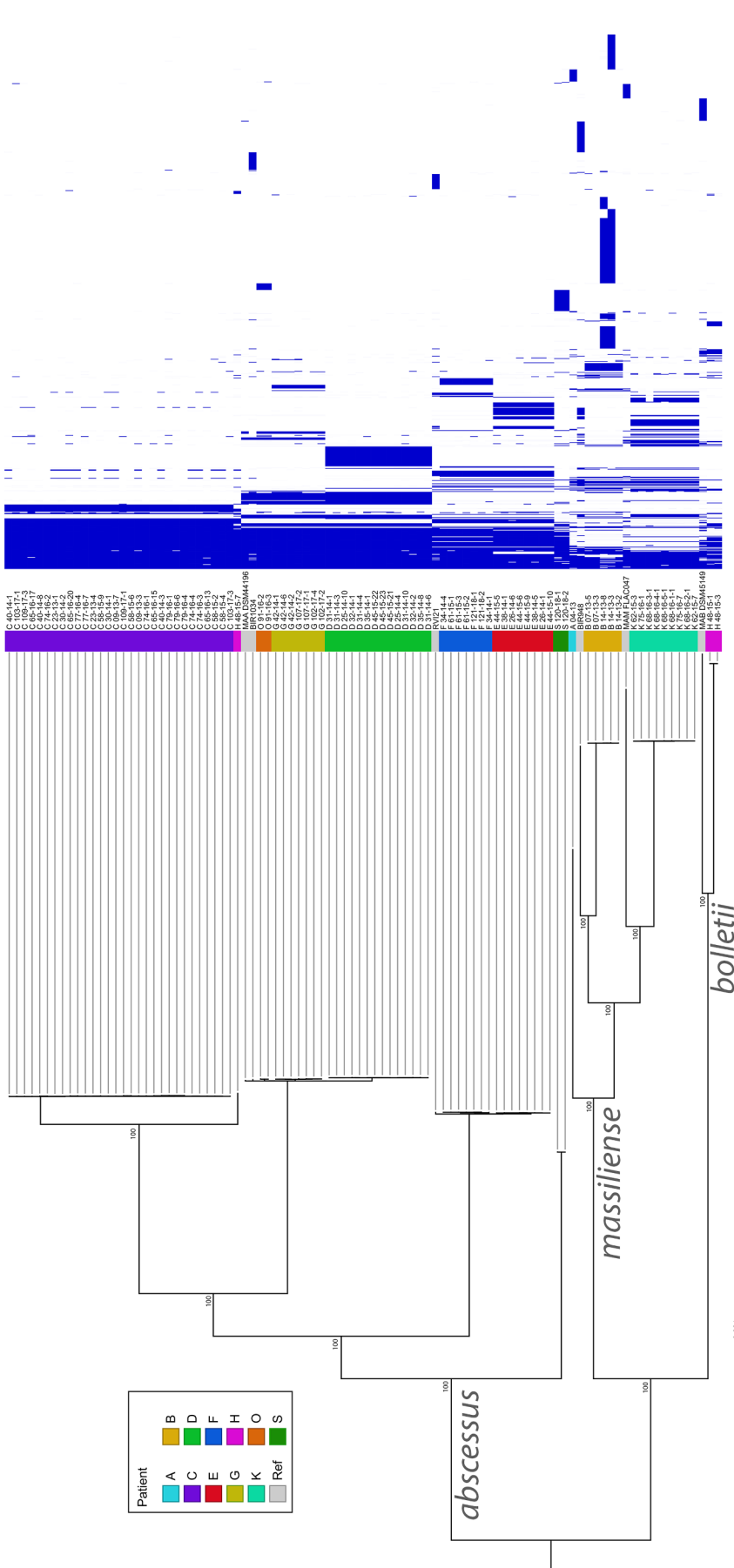
Figure 1. Phandango illustration showing a core genome-based Maximum likelihood tree corrected for recombination events of 88 *M. abscessus* isolates from 11 CF patients and the accessory genome. On the left side the Maximum likelihood tree is shown, on the right-side accessory gene presence in the respective isolates is indicated by blue lines. Patients providing samples are named by letters (A to S). Names of *M. abscessus* isolates are composed as follows: first letter stands for patient, first number for the sample number, second number for the year of isolation, last number for the colony number. Reference strains included in the tree were DSM 44196 (= ATCC 19977) for *M. abscessus abscessus* (accession NC_010397.1), CIP 108541 for *M. abscessus bolletii* (accession NZ_JRMF00000000.1) and FLAC047 for *M. abscessus massiliense* (accession NZ_CP021122.1). Representatives of the global patient-transmissible clusters [BIR 948 (accession ERS383065), RVI 21 (accession ERS244779), BIR 1034 (accession ERS383155)] described in [6] were included to identify global cluster strains present in the collection of CF isolates.

treatment center. Absence of patient-to-patient transmission was further confirmed by considerable differences in the accessory genomes (Figure 1).

Genetic diversity evolving during persistent MABSa infection

The longest tracking time and highest sample numbers were obtained for patient C. We chose isolates from this patient for analysis of in-patient diversity of MABS. The first respiratory sample obtained from this patient was taken in the month after diagnosis of MABS infection, followed by samples after five, 10, 18, 26, 32, 34, 36, 38, 49 and 53 months. Between two to four colonies per sample were included in the analysis. In total, 30 isolates from 11 serial respiratory samples collected over 4.5 years were gained. Table 1 shows the sampling time points (in months after NTM-diagnosis), the colony morphotype of isolates, clinical disease parameters (BMI, FEV1) and the antibiotic treatment. The patient was infected with *Pseudomonas* during the whole study period.

All 30 isolates were sequenced by Illumina technology (Supplementary Table S3, Figure 1 and Supplementary Figure S1). The Maximum Likelihood Tree in Figure 1 shows that these isolates form a cluster separated from the isolates from the other patients. One of the isolates obtained from the first sample (isolate 09–13-3) was additionally sequenced by MinION technology to complete the genome and provide a baseline reference for further analysis. Supplementary Table S4 summarizes the statistics for genome sequence assembly of the completed genome from isolate 09-13-3. The genome from isolate 09-13-3 comprised a chromosome of a size of 4.949.160 bp and a plasmid of 24.978 bp. This plasmid (pMabs-09-13, plasmid map in Supplementary Figure S2 A) exhibits an identity of 99.86% (with a coverage of 100%) to plasmids pGD42-1 (accession CP065281.1), pGD69A-1 (accession CP065270.1), and pGD69B-1 (accession CP065267.1) described by Dedrick et al. [24]. Supplementary Figure S2 B shows an alignment of plasmids pMabs-09-13 and pGD42-1.

SNV calling using the MinION genome sequence from 09-13-3 as baseline was applied to identify gene variations occurring in this patient over the 4.5-years monitoring period. Only non-synonymous (ns) SNVs and larger deletions as well as mutations in the rRNA genes were further considered. Fifty-three genes exhibiting non-synonymous mutations with respect to isolate 09–13-3 were identified. These genes and the affected isolates are listed in Table 2.

A visualization of the frequency and chronology of chromosomal gene mutations occurring in 29 isolates compared to the reference 09–13-3 is provided in Figure 2. The number of genes with non-synonymous mutations was higher from 18 months after MABS diagnosis compared to the period before. Occurrence of dominating clones exhibiting and sustaining specific combinations of mutations was not observed during the observation time period. However, a clear trend was observed with respect to the loss of the plasmid pMabs-09-13 over time. The strain 09–13-3 originally contained a plasmid of a size of 24.978 bp (Supplementary Figure S2). This plasmid was lost from the MABS strain in the course of chronic infection. Specifically, all isolates contained the plasmid until ten months after MABS diagnosis. However, it remained absent in all isolates sampled at and after 38 months.

Network analysis with the set of mutated genes by STRING (https://string-db.org/) identified ten functionally enriched PFAM protein domains (Table 3).

Functionally enriched genes comprised a cluster involved in cell wall synthesis and resistance toward ethambutol (*embA* and *embC*) and a cluster involved in synthesis of glycopeptidolipids (GPL) (*eryA*, *mps2* and *mps1*). Also, MAB_4690c belonging to a second GPL-like gene cluster from MABS [50] was among the functionally enriched genes as well as MAB_2255 and MAB_2256, which also encode a probable non-ribosomal peptide synthetase and a probable polyketide synthase. Furthermore, *betA* (probable glucose-methanol-choline oxidoreductase) and *choD* (putative cholesterol oxidase) were among enriched genes.

The mutations in the GPL synthesis genes [53] can explain the rough morphotype of all rough isolates. Confirmation of the impact of mutations in GPL synthesis genes on GLP composition was obtained by thin layer chromatography (TLC) with GPL extracted from a smooth and four rough isolates exhibiting different types of mutations (Supplementary Figure S3).

Comparison of MICs from ten rough and ten smooth paired isolates originating from the same respiratory samples showed different median MICs for Amikacin, Cefoxitin, Imipenem and Linezolid. Interestingly, rough colonies showed higher median MIC values to three of these antibiotics (Amikacin, Cefoxitin and Imipenem), while they exhibited a lower median MIC to one of them (Linezolid) (Figure 3). Additional information on MICs of MABS isolated from patient C is provided in Supplementary Table S5.

Diversification in virulence- and resistance associated genes during chronic lung infection

Out of the 53 genes that had developed non-synonymous gene variations, at least 17 genes or their homologs in other mycobacteria were published to be involved in mycobacterial virulence (Table 2). These genes or their homologs exert an impact (i) on survival in the host or host cells [MAB_0033c (*pknB*),

Table 1 Chronology of *M. abscessus* isolation from respiratory samples from patient C, clinical disease parameters, and antibiotic treatment.

Months after diagnosis	Isolate	Colony morphology	BMI	FEV1[1]	Administered antibiotics
1	09–13–3	smooth	15,9	77,9	
	09–13–7	smooth			
5	23–13–1	smooth	15,9	77,0	Cotrimoxazole, Clarithromycin, Minocycline, Moxifloxacin (oral)
	23–13–4	smooth			
10	30–14–1	smooth	15,0	65,0	Clarithromycin, Minocycline oral Amikacin (nebulized)
	30–14–2	smooth			
18	40–14–1	rough	16,2	68,0	Amikacin (iv) Azithromycin, Linezolid (oral)
	40–14–3	smooth			
	40–14–8	smooth			
26	58–15–2	rough	14,8	53,0	
	58–15–4	rough			
	58–15–6	smooth			
	58–15–9	smooth			
32	65–16–13	smooth	16,0	64,0	Amikacin, Cefoxitin (iv) Ciprofloxacin, Minocycline (oral)
	65–16–15	smooth			
	65–16–17	rough			
	65–16–20	rough			
34	74–16–1	smooth	16,0	64,0	Cefoxitin (iv) Ciprofloxacin, Clofazimine, Azithromycin (oral)
	74–16–2	smooth			
	74–16–3	rough			
	74–16–4	rough			
36	77–16–4	smooth	16,2	62,0	Cefoxitin (iv) Ciprofloxacin, Clofazimine, Azithromycin (oral)
	77–16–7	smooth			
38	79–16–1	rough	15,8	47,0	Cefoxitin (iv) Ciprofloxacin, Clofazimine, Azithromycin (oral)
	79–16–4	smooth			
	79–16–6	smooth			
49	103–17–1	smooth	14,2	41,0	Cefoxitin (iv) Ciprofloxacin, Clofazimine, Azithromycin (oral)
	103–17–3	rough			
53	109–17–1	rough	14,9	46,0	Cefoxitin (iv) Ciprofloxacin, Clofazimine, Azithromycin (oral)
	109–17–3	smooth			

BMI: Body mass index; FEV1: Forced expiratory volume per second. [1]% of predicted.

Table 2 nsSNVs and larger deletions in 29 isolates from 11 serial samples obtained over 4.5 years from a chronically infected patient. Shown are the locus tags of the homologous genes in the reference strain ATCC 19977, the locus tags in the completed genome from the first sample (09–13-3), gene names, annotations, functional COG categories and names of the isolates exhibiting the mutations when compared to the initial isolate 09–13-3. Known associations to virulence and resistance of the genes or homologous genes in other mycobacterial species are indicated in the last two columns.

Locus tag in ATCC 19977[1]	Locus tag in 09-13-3[2]	Gene name[3]	Annotation[3]	Functional category[4]	Isolates exhibiting SNVs[5]	Association of gene to virulence	Association of gene to resistance
MAB_0033c	HIFIHNKG_00044	pknB	Probable serine/threonine kinase PknB	[K] [L] [T]	109–17-3	Survival in the host [25]	ß-lactam, Rifampin [26]
MAB_0173	HIFIHNKG_00191		UbiA prenyltransferse family protein	[H]	65–15-13		Ethambutol [27]
MAB_0186c	HIFIHNKG_00204	embA	Probable arabinosyltransferase A	[M]	65–16-15		Ethambutol [27,28]
MAB_0189c	HIFIHNKG_00207	embC	Probable arabinosyltransferase C	[M]	30–14-1, 40–14-3, 40–14-8, 58–15-2, 58–15-6, 58–15-9, 65–16-17, 65–16-20, 74–16-1, 74–16-2, 74–16-3, 74–16-4, 77–16-4, 79–16-1, 79–16-4, 79–16-6, 103–17-1	LAM biosynthesis [29]	Ethambutol [29]
No homolog MAB_0277c	HIFIHNKG_00238 HIFIHNKG_00346	tcyB	Hypothetical protein Probable amino acid ABC transporter permease	[E] [P] [T]	58–15-4 65–16-20		
MAB_0310c	HIFIHNKG_00380		Putative cyclopropane-fatty-acyl-phospholipid synthase	[M]	79–16-4	Survival in the host [30]	
MAB_0315	HIFIHNKG_00385	hsaA	Flavin-dependent monooxygenase, oxygenase subunit HsaA	[I]	40–14-1		
MAB_0415, MAB_0416c	HIFIHNKG_00492, HIFIHNKG_00493	crp	Putative Crp/Fnr-family transcriptional regulator, cAMP-binding protein	[E] [G] [K] [T]	40–14-1, 74_16_2, 79–16-1, 79–16-4, 79–16-6		Clofazimine [31]
MAB_0673	HIFIHNKG_00715	tcrX	Putative DNA-binding response regulator PhoP	[K] [T]	65–16-15	Iron acquisition [32]; Virulence [33]	
MAB_0816	HIFIHNKG_00859	betA	Probable glucose-methanol-choline oxidoreductase	[E]	74–16-2, 79–16-1, 79–16-4, 79–16-6		
MAB_0939	HIFIHNKG_00948	eryA	Probable polyketide synthase, Malonyl CoA-acyl carrier proteintransacylase	[Q]	40–14-3	Virulence [34,35]	Amikacin, Cefoxitin, Imipenem, Linezolid [this study]
MAB_1080	HIFIHNKG_01092	mspD	porin	[S]	58–15-2, 103–17-3, 109–17-1	Iron acquisition [36]; Zinc acquisition [37]; Intracellular survival [38]	Fluoroquinolone, Chloramphenicol [39]; Clarithromycin [40]
MAB_1129	HIFIHNKG_01124	tatD yabD	Probable deoxyribonuclease	[L]	58–15-9		
MAB_1156c	HIFIHNKG_01160	lysA	Diaminopimelate decarboxylase LysA	[E]	77–16-4		
MAB_1499	HIFIHNKG_01502		Putative FAD dependent oxidoreductase	[E]	74–16-3, 74–16-4	Virulence [41]	
MAB_1539c	HIFIHNKG_01542		Mycobacterium membrane protein	[S]	103–17-1		
MAB_1607	HIFIHNKG_01626	rnE	Possible ribonuclease E	[J]	103–17-3		
MAB_1678c	HIFIHNKG_01697	furB	Putative ferric uptake regulator FurB	[P]	103–17-3, 109–17-1	Zn acquisition [42]	

(Continued)

Table 2 (Continued).

Locus tag in ATCC 19977[1]	Locus tag in 09-13-3[2]	Gene name[3]	Annotation[3]	Functional category[4]	Isolates exhibiting SNVs[5]	Association of gene to virulence	Association of gene to resistance
MAB_1881c	HIFIHNKG_01794		Putative transcriptional regulator, TetR family	[K]	09-13-7, 23-13-1, 23-13-4, 30-14-1, 30-14-2, 40-14-1, 40-14-3, 40-14-8, 58-15-2, 58-15-4, 58-15-6, 58-15-9, 65-16-13, 65-16-15, 65-16-17, 65-16-20, 74-16-1, 74-16-2, 74-16-3, 74-16-4, 77-16-4, 77-16-7, 79-16-1, 79-16-4, 79-16-6, 103-17-1, 103-17-3, 109-17-1		Clarithromycin [40]
MAB1991c	HIFIHNKG_01937	mptA	Integral membrane protein Alpha-(1-6-mannopyranosyltransferase A	[S]	103-17-3, 109-17-1	LM/LAM synthesis [43]	
MAB_2161c	HIFIHNKG_02096		Hypothetical low molecular weight antigen Mtb12	[S]	09-13-7		
MAB_2255	HIFIHNKG_02189		Probable non-ribosomal peptide synthetase	[Q]	109-17-3		
MAB_2256	HIFIHNKG_02190		Probable polyketide synthase	[Q]	103-17-3		
MAB_2299c	HIFIHNKG_02233		Possible transcriptional regulatory protein	[K]	79-16-4		Clofazimine, Bedaquiline [31,44]
MAB_2570c	HIFIHNKG_02505	mmpL	Probable membrane protein, MmpL family	[D]	65-16-20, 77-16-4	Transport of cell wall lipids [45]	Antibiotics [45]
MAB_2645c	HIFIHNKG_02588	trpC	Indole-3-glycerol-phosphate synthase	[E]	74-16-3, 74-16-4	Survival in host cells [46]	
MAB_2679	HIFIHNKG_02622		Uncharacterized protein	[S]	74-16-1		
MAB_2788	HIFIHNKG_02733	ggtB	Gamma-glutamyl-transpeptidase	[E]	77-16-4	Survival in host cells [47]	
MAB_2825	HIFIHNKG_02770		Acetyltransferase family protein	[I]	103-17-3		
No homolog	HIFIHNKG_02868		Hypothetical protein	[I]	40-14-1		
MAB_3029	HIFIHNKG_02972	ideR	Iron-dependent repressor	[K]	65-16-20, 77-16-4	Iron acquisition [48]	
MAB_3034	HIFIHNKG_02977		Alpha/beta hydrolase fold family hydrolase	[I]	65-16-20, 77-16-4		
MAB_3036c	HIFIHNKG_02979	nrdR	Transcriptional repressor NrdR	[K]	40-14-3		
MAB_3404c	HIFIHNKG_03344	nrdF	Ribonucleoside-diphosphate reductase subunit beta	[F]	74-16-1, 103-17-1		
No homolog	HIFIHNKG_03363		Hypothetical protein	[S]	74-16-3		
No homolog	HIFIHNKG_03364		Hypothetical protein	[S]	74-16-3, 74-16-4		
MAB_3623	HIFIHNKG_03588		Probable transcriptional regulatory protein, AraC family	[K]	65-16-20		
No homolog	HIFIHNKG_03589		Hypothetical Gtr-like protein	[I] [M] [S]	77-16-7, 109-17-3		
MAB_3669	HIFIHNKG_03634		Uncharacterized protein	[S]	40-14-8		
MAB_3698	HIFIHNKG_03662		Putative ABC transporter	[T] [V]	40-14-3, 40-14-8, 58-15-2, 74-16-2, 79-16-1, 79-16-4, 79-16-6		
MAB_3719c	HIFIHNKG_03684	choD	Putative cholesterol oxidase ChoD	[E]	103-17-3, 109-17-1	Survival in host cells [49]	
MAB_4098c	HIFIHNKG_04080	mps2, lgrD_2	Probable peptide synthetase NRP	[Q]	58-15-4, 103-17-3, 109-17-1	Virulence [35,50]	Amikacin, Cefoxitin, Imipenem, Linezolid [this study]
MAB_4099c	HIFIHNKG_04081	mps1, lgrC_1	Probable non-ribosomal peptide synthetase	[Q]	58-15-2, 65-16-17, 65-16-20, 74-16-3, 74-16-4, 79-16-1	Virulence [35,50]	Amikacin, Cefoxitin, Imipenem, Linezolid [this study]; Clofazimine [31]
MAB_4103c	HIFIHNKG_04086		Probable methyltransferase	[Q]	74-16-3, 74-16-4	Virulence [51]	

(Continued)

Table 2 (Continued).

Locus tag in ATCC 19977[1]	Locus tag in 09–13-3[2]	Gene name[3]	Annotation[3]	Functional category[4]	Isolates exhibiting SNVs[5]	Association of gene to virulence	Association of gene to resistance
MAB_4105c	HIFIHNKG_04088	mtfD	Methyltransferase	[E] [S]	74–16-3, 74–16-4		
MAB_4320c	HIFIHNKG_04305		Putative TetR transcriptional regulator	[K]	103–17-3		
MAB_4372	HIFIHNKG_04358		Putative 3-(2,3-dihydroxyphenyl) propionic acid dioxygenase	[S]	58–15-2		
MAB_4654	HIFIHNKG_04625	mauC	Conserved hypothetical protein (plastocyanin-like)	[C]	74–16-3, 74–16-4		
MAB_4690c	HIFIHNKG_04663	lgrC_2	Probable non-ribosomal peptide synthetase PstA, Linear gramicidin synthase subunit C	[Q]	65–16-17		
MAB_4695c	HIFIHNKG_04668		Putative glycosyltransferase/ rhamnosyltransferase	[C] [G]	65–16-20		
MAB_4760	HIFIHNKG_04733	nox	Probable nitroreductase	[C]	109–17-3, 103–17-3, 109–17-1		
MAB_r5052		rrl	23S rRNA				Clarithromycin [52]

[1]accession: NC010397.1; [2] accession: ERS4791737; [3] according to NCBI (https://www.ncbi.nlm.nih.gov/), STRING (https://string-db.org/), Uniprot (https://www.uniprot.org/); [4] according to EggNOG (http://eggnog5.embl.de/#/app/seqscan). [5] See Supplementary Table S3 for details of isolates. [4] COG categories are: [C] Energy production and conversion, [D] Cell cycle control, cell division, chromosome partitioning, [E] Amino acid transport and metabolism, [F] Nucleotide transport and metabolism, [G] Carbohydrate transport and metabolism, [H] Coenzyme transport and metabolism, [I] Lipid transport and metabolism, [J] Translation, ribosomal structure and biogenesis, [K] Transcription, [L] Replication, recombination and repair, [M] Cell wall/membrane/envelope biogenesis, [P] Inorganic ion transport and metabolism, [Q] Secondary metabolites biosynthesis, transport and catabolism, [S] Function unknown, [T] Signal transduction mechanisms, [V] Defense mechanisms. nsSNV: non-synonymous small nucleotide variation.
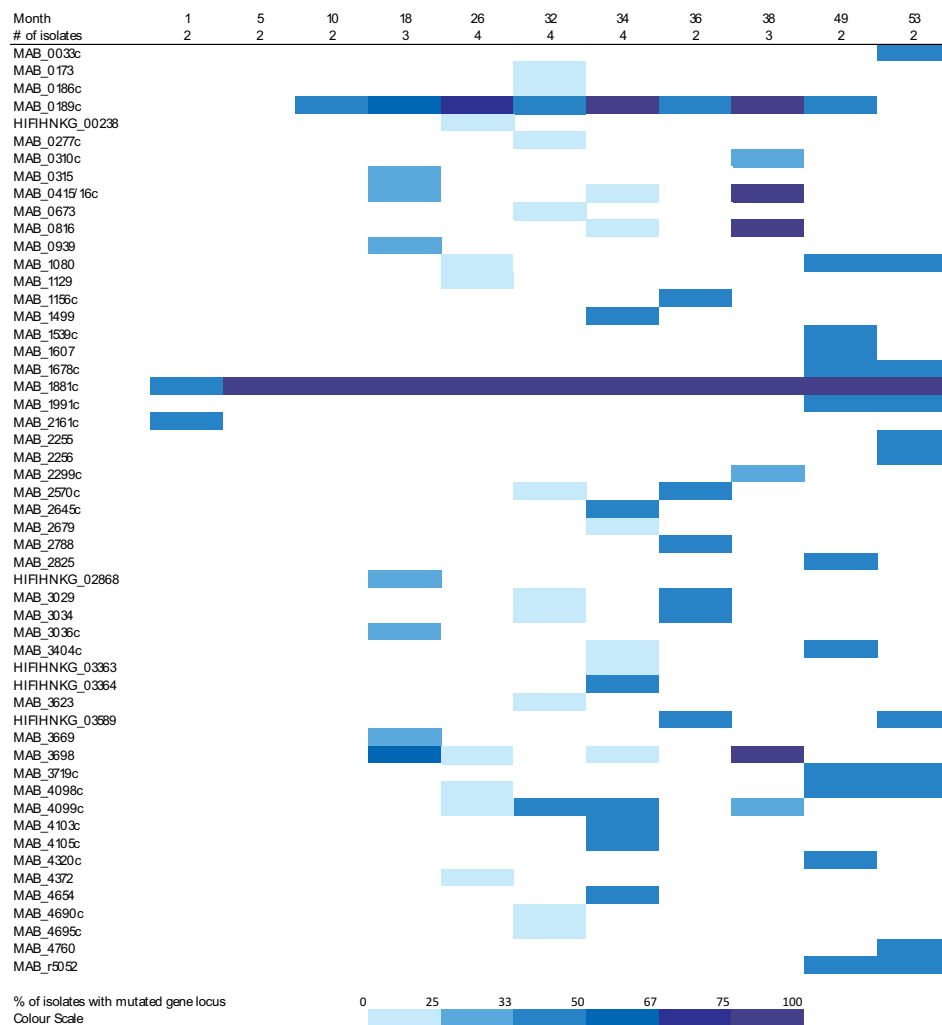
Figure 2. Chronology of occurrence of non-synonymous chromosomal mutations in *M. abscessus* isolated during 4.5 years from patient C. The upper line shows the timepoints of sampling in months after first diagnosis of *M. abscessus* infection. The line below indicates the number of isolates sequenced from these samples. In the lower part on the left, the genes exhibiting non-synonymous mutations in any of the isolates are listed. On the right, the percentage of isolates with non-synonymous mutations in the specific genes is visualized by color depth according to the color scale shown below.

Table 3 Enrichment of PFAM protein domains in the pool of genes displaying non-synonymous mutations in the *M. abscessus* isolates from patient C according to STRING network analysis.

PFAM Protein domain and term description	Matching proteins[1]	False discovery rate
PF00550 Phosphopantetheine attachment site	MAB_0939 (*eryA*), MAB_2255, MAB_2256, MAB_4690c (*lgr_C2*), MAB_4099c (*lgrC_1*), MAB_4098c (*lgrD_2*)	7.23×10^{-5}
PF00668 Condensation domain	MAB_2255, MAB_4098c (*lgrD_2*), MAB_4099c (*lgrC_1*), MAB_4690c (*lgr_C2*)	0.00093
PF13193 AMP-binding enzyme C-terminal domain	MAB_2255, MAB_4098c (*lgrD_2*), MAB_4099c (*lgrC_1*), MAB_4690c (*lgr_C2*)	0.0153
PF04602 Mycobacterial cell wall arabinan synthesis protein	MAB_0186c (*embA*), MAB_0189c (*embC*)	0.0164
PF14896 EmbC C-terminal domain	MAB_0186c (*embA*), MAB_0189c (*embC*)	0.0164
PF00732 GMC oxidoreductase	MAB_0816 (*betA_1*), MAB_3719c (*choD*)	0.0227
PF05199 GMC oxidoreductase	MAB_0816 (*betA_1*), MAB_3719c (*choD*)	0.0227
PF00501 AMP-binding enzyme	MAB_2255, MAB_4098c (*lgrD_2*), MAB_4099c (*lgrC_1*), MAB_4690c (*lgr_C2*)	0.0264
PF16197 Ketoacyl-synthetase C-terminal extension	MAB_0939 (*eryA*), MAB_2256	0.0264
PF00698 Acyl transferase domain	MAB_0939 (*eryA*), MAB_2256	0.0488

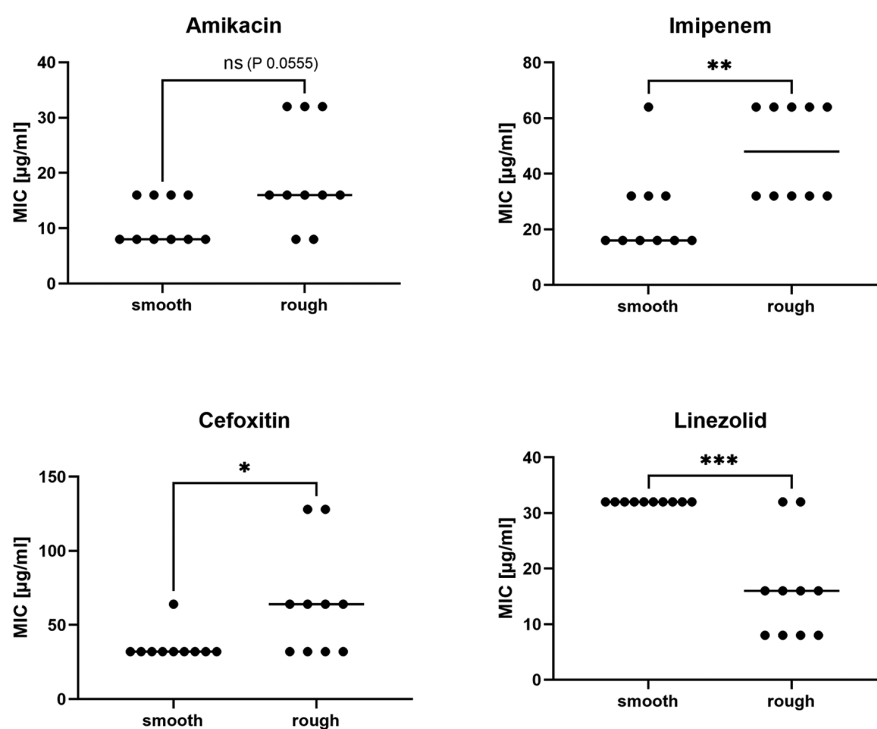[1]Locus tags (gene names) of the homologs in the reference strain ATCC 19977.

Figure 3. Comparison of MICs from smooth and rough isolates from patient C. Ten smooth and ten rough *M. abscessus* isolates from nine serial respiratory samples were tested using the Sensititre system (TREK diagnostics system, ThermoFisher Scientific). Out of the 13 antibiotics available in the sensititre panel three (Cefoxitin, Imipenem and Linezolid) showed statistically significant differences in MIC between the smooth and rough isolates from this patient (Mann Whitney Test, *: P < 0.05, **: P < 0.01, ***: P < 0.001). Bars indicate the median values.

MAB_0310c, MAB_1080 (porin), MAB_2645c (*trpC*), MAB_2788 (*ggtB*) MAB_3719c (*choD*)], (ii) on cell wall synthesis [MAB_0189c (*embC*), MAB_1991c (*mptA*), MAB_2570c (*mmpL*)], (iii) on iron and zinc acquisition [MAB_0673 (*tcrX*), MAB_1080 (porin), MAB_1678c (*furB*), MAB_3029 (*ideR*)], and (iv) on GPL synthesis [MAB_0939 (*eryA*), MAB_4098c (*mps2*), MAB_4099c (*mps1*)]. References are provided in Table 2.

Thirteen of the 53 MABS genes or their homologs in other mycobacterial species are known to be related to antibiotic resistance (Table 2). It has been shown that genes or homologs in other mycobacteria to MAB_0173, MAB_0186c (*embA*), and 0189c (*embC*) are related to Ethambutol resistance. Clofazimine resistance was associated to genes MAB_0146c (*crp*), MAB_2299c, and MAB_4099c (*mps1*). MAB_2299c had additionally been associated with Bedaquiline resistance. Mycobacterial porin genes such as MAB_1080 were related to resistance toward Fluoroquinolone, Chloramphenicol and Clarithromycin. Clarithromycin resistance may additionally be influenced by gene MAB_1881c and *rrl*. The mutation that was identified in the *rrl* gene (position 2270, A/C) is known to confer acquired Clarithromycin resistance.

PknB from mycobacteria was shown to impact resistance toward ß-lactams and Rifampin. References are provided in Table 2.

Discussion

MABS is a highly problematic multi-drug resistant pathogen. Despite protracted combination therapy accompanied by severe side effects, only low conversion rates of typically 40–50% are reported [8] calling for more personalized treatment and also consideration of the mycobacterial population dynamics. Accordingly, the present study focused on exploring the strategy of chronic MABS to adapt to the lung environment in CF patients.

MABS predominated NTM infections in our study group, followed by MAH. The MABS subspecies distribution with 63.6% of subspecies *abscessus*, 27.3% of subspecies *massiliense* and 9% of subspecies *bolletii* was highly similar to the distribution found in the global study from Bryant et al [6].

Five of the eleven MABS-infected patients carried strains belonging to one of three global human transmissible clusters, that have been reported to be more virulent and

resistant and at the same time more frequently associated with chronic disease compared to sporadic strains [6]. Nevertheless, the results from the SNP analysis argued against transmission of MABS between patients in the study group. This was additionally supported by comparison of the accessory genomes of the isolates. Comparison of accessory genomes for discrimination of closely related MABS isolates was also proposed by Davidson [54] and Doyle and colleagues [55]. There is meanwhile a greater number of publications (e.g [55,56,57]) reporting the presence of global cluster strains in patient cohorts without epidemiologic evidence for transmission among patients. The absence of patient-to-patient transmission endorses infection control measures in the CF center in Berlin which involve among others spatial and/or temporal separation of patients with NTM in respiratory tract and wearing a face mask during the entire clinical stay [58].

Comparative genome analysis of 30 isolates from 11 serial samples from a chronically infected patient identified 53 genes with non-synonymous variations. Although colony picking did not allow representation of the whole MABS population in the samples, it enabled us to identify mutations and their temporal appearance during chronic infection. Additional to chromosomal mutations, the plasmid from this strain present in the beginning was lost during persistent infection. This may be explained by the fitness cost of plasmid maintenance in stress conditions present in the human host and is in good accordance to a study by Shoulah et al. [59], who found more plasmid-derived genes in environmental compared to clinical isolates from MAH. Associations between molecular changes (Table 2) and antibiotic treatment as well as clinical disease progression (Table 1) were not evident, which could be due to the multifactorial character of CF disease and the fact that the collection of sequenced isolates represents only a portion of derivatives present in the lung of the patient. Also, by sequencing of isolates from different body sites, Shaw and colleagues (2019) [9] had shown that sputum did not completely reflect in-patient diversity of MABS and also did not represent the overall antibiotic resistance profiles.

Isolates with mutations in these 53 genes are extremely valuable to study virulence and resistance mechanisms of persistent MABS, which are currently insufficiently investigated. Frequent genetic changes included those leading to GPL deficiency and rough colony morphotype. These mutations were associated with increased MICs for Amikacin, Cefoxitin and Imipenem and decreased MIC for Linezolid. In contrast to the present study comparing MICs of isogenic isolates, previous studies on strains isolated from different patients let to controversial outcomes [60,61]. Our study emphasizes the need to give more attention to the impact of morphotypes on drug resistance when searching for new anti-mycobacterial drugs.

Of the 53 genes exhibiting genetic diversity, at least 23 genes or their homologs in other mycobacteria have been assigned to be virulence- and/or resistance-associated. Genetic diversity evolved in genes related to resistance to Ethambutol, Rifampin, Clofazimine, Bedaquiline, Fluoroquinolone, Chloramphenicol, Imipenem, Cefoxitin and Clarithromycin. Two isolates had acquired the A to C mutation at position 2270 (MABS numbering) in the *rrl* gene, a mutation known to confer acquired Clarithromycin resistance [62]. Mutations in *rrl* and *furB* were also found to exhibit in-patient diversity by Shaw et al. (2019) [9]. Our study very well complements their results. Shaw et al. took samples during a relatively short-time period and in the specific situation after lung transplantation. The big advantage of their study was the sampling of different body sites, enabling a more complete picture of in-patient diversity. On the other side, our study although limited to respiratory isolates, is prior when considering the long sampling period of 4.5 years that very well reflects mutation events owing to a chronic course of disease. Further, the study by Bryant et al. (2021) [10], confirms the relevance of genes exhibiting diversity as identified in the present study. Out of the 53 genes identified, six genes (*rrl*, GPL synthesis genes, *ubiA*, *crp/fnr*, *tetR*, and *ideR*) were found by Bryant et al. to exhibit in-patient diversity. Three of these (*ubiA*, *crp/fnr*, and *ideR*) were shown to be involved in intracellular survival [10].

Interestingly, our results demonstrate that in-patient evolution did not bring forth fewer dominating sub-populations but rather fostered the coexistence of diverse mutant sub-populations.

We aimed to estimate the mutation rate of isolates from patient C using tip dating. However, when implementing two statistical tests, we failed at detecting a temporal signal in our sequences, precluding any meaningful rate assessment (data not shown).

The upsurge of genetic diversity possibly enables the population to adapt to changing living conditions as illustrated by the following example. MAB ecology combines the ability to survive both in the environment and in human airways, which offer disparate access to biometals such as zinc and iron. Such metals are, on the one hand, essential cofactors of enzymes and structural components of regulatory proteins. On the other hand, however, excessive concentrations thereof can be toxic. Therefore, a stringent regulatory system for homeostasis is required. The sputum from CF patients displays highly enriched metal concentrations of zinc and iron [63], which may favor genetic diversity within genes involved in zinc and iron homeostasis during chronic infection. Zinc uptake in mycobacteria is regulated by *zur-smtB*. Among the genes exhibiting gene

diversity in persistent infection, *zur* is a zinc-binding repressor controlling genes involved in zinc uptake [37]. The porin MspD was shown to be induced by zinc starvation or *zur* deletion [37]. Moreover, MAB_1080, which was annotated as the porin protein MspD, was also among the genes exhibiting diversity upon chronic infection. Mutations were also identified in *ideR*, a gene that regulates transcription in response to iron levels [64], as well as in *tcrX*, which was shown to be up-regulated when *M. tuberculosis* was grown under iron-limited conditions [32]. Furthermore, Msp porins of rapid growing mycobacteria promote growth in nutrient-limited conditions by enhancing diffusion of small hydrophilic molecules into the cells. At the same time, however, they limit intracellular survival by increasing vulnerability to killing by reactive nitrogen [38,65]. Therefore, the mutation in MAB_1080 may additionally impact the survival of MABS in macrophages.

ChoD, a cholesterol oxidase, is needed in *M. tuberculosis* survival in macrophages [49]. A mutant deficient in the gamma-glutamyl-transpeptidase (GgtB) from *M. tuberculosis*, which is homologous to MAB_2788, was shown to be resistant to the toxic effects of Glutathione/S-nitrosoglutathione and therefore better survived in macrophages [47]. Macrophages are not the only host cells for mycobacteria, some of which are also able to replicate in Type II alveolar epithelial cells (AECs). The tryptophan synthesis gene *trpC* from *M. tuberculosis* is strongly up-regulated during growth in AECs [46] and also the homologue from this gene was mutated in two of the MABS isolates.

MptA, EmbC and MmpL family proteins are involved in lipid/glycolipid synthesis. MptA is a mannosyltransferase necessary for synthesis of the mannan backbone from Lipomannan. EmbC from *M. tuberculosis* catalyses arabinosylation of Lipomannan to form Lipoarabinomannan (LAM), which is involved in immune response by interacting with TLR2 and mannose-receptor [29,43,66]. Interestingly, a longitudinal analysis by Kreutzfeld [67] of 6 MABS *bolletii* isolates from a CF patient collected over 11 years also identified mutations in the *embABC* operon during chronic infection.

In conclusion, our data indicate that the survival strategy of MABS in the CF lung is not toward the clonal expansion of few dominant variants but the preservation of heterogeneous subpopulations allowing adaptation to changing lung conditions. Similar future longitudinal studies involving other MABS strains and patients and including samples from different body sites [9] will further explore the range of variation of MABS in-patient evolution during chronic lung infection, which in future will facilitate the development of efficient treatment options.

Data availability statement

All genome sequences have been submitted to the European Nucleotide Archive (URL: https://www.ebi.ac.uk/ena/browser/view/PRJEB39129?show=reads).

Data deposition

Genome sequences are deposited at the European Nucleotide Archive (ENA).

Ethical statement

Permission for the study was obtained from the ethics committee of the Charité –Universitätsmedizin Berlin (EA2/093/12). Written consent had been obtained from all patients.

Statement to health and safety regulations:

The authors confirm compliance with national health and safety regulations.

ORCID

Astrid Lewin http://orcid.org/0000-0002-9051-9935
Carsten Schwarz http://orcid.org/0000-0003-3474-2857

References

[1] Heifets L. Mycobacterial infections caused by nontuberculous mycobacteria. Semin Respir Crit Care Med. 2004;25(3):283–295.
[2] Johnson MM, Odell JA. Nontuberculous mycobacterial pulmonary infections. J Thorac Dis. 2014;6(3):210–220.

[3] Martiniano SL, Nick JA, Daley CL. Nontuberculous mycobacterial infections in cystic fibrosis. Clin Chest Med. 2016;37(1):83–96.

[4] Esther CR Jr., Esserman DA, Gilligan P, et al. Chronic Mycobacterium abscessus infection and lung function decline in cystic fibrosis. J Cystic Fibrosis. 2010;9 (2):117–123.

[5] Lynch JP 3rd, Sayah DM, Belperio JA, et al. Lung transplantation for cystic fibrosis: results, indications, complications, and controversies. Semin Respir Crit Care Med. 2015;36(2):299–320.

[6] Bryant JM, Grogono DM, Rodriguez-Rincon D, et al. Emergence and spread of a human-transmissible multidrug-resistant nontuberculous Mycobacterium. Science. 2016;354(6313):751–757.

[7] Nessar R, Cambau E, Reyrat JM, et al. Mycobacterium abscessus: a new antibiotic nightmare. J Antimicrob Chemother. 2012;67(4):810–818.

[8] Martiniano SL, Davidson RM, Nick JA. Nontuberculous mycobacteria in cystic fibrosis: updates and the path forward. Pediatr Pulmonol. 2017;52(S48):S29–S36.

[9] Shaw LP, Doyle RM, Kavaliunaite E, et al. Children with cystic fibrosis are infected with multiple subpopulations of Mycobacterium abscessus with different antimicrobial resistance profiles. Clin Infect Dis. 2019;69(10):1678–1686.

[10] Bryant JM, Brown KP, Burbaud S, et al. Stepwise pathogenic evolution of Mycobacterium abscessus. Science. 2021;372(6541):eabb8699.

[11] Ruangkiattikul N, Rys D, Abdissa K, et al. Type I interferon induced by TLR2-TLR4-MyD88-TRIF-IRF3 controls Mycobacterium abscessus subsp. abscessus persistence in murine macrophages via nitric oxide. Int J Med Microbiol. 2019;309(5):307–318.

[12] Woods GL, Brown-Elliot BA, Conville PS, et al. Susceptibility testing of mycobacteria, nocardiae, and other aerobic actinomycetes. **2nd edition**. Clinical and Laboratory Standards Institute; Pennsylvania USA; 2011.

[13] Bolger AM, Lohse M, Usadel B. Trimmomatic: a flexible trimmer for Illumina sequence data. Bioinformatics. 2014;30(15):2114–2120.

[14] Seemann T. Prokka: rapid prokaryotic genome annotation. Bioinformatics. 2014;30(14):2068–2069.

[15] von Mentzer A, Connor TR, Wieler LH, et al. Identification of enterotoxigenic Escherichia coli (ETEC) clades with long-term global distribution. Nat Genet. 2014;46(12):1321–1326.

[16] Stamatakis A. RAxML version 8: a tool for phylogenetic analysis and post-analysis of large phylogenies. Bioinformatics. 2014;30(9):1312–1313.

[17] Didelot X, Wilson DJ, Prlic A. ClonalFrameML: efficient inference of recombination in whole bacterial genomes. PLoS Comput Biol. 2015;11(2):e1004041.

[18] Hadfield J, Croucher NJ, Goater RJ, et al. Phandango: an interactive viewer for bacterial population genomics. Bioinformatics. 2018;34(2):292–293.

[19] Wick RR, Judd LM, Holt KE. Deepbinner: demultiplexing barcoded Oxford Nanopore reads with deep convolutional neural networks. PLoS Comput Biol. 2018;14(11):e1006583.

[20] Leger A, Leonardi T. pycoQC, interactive quality control for Oxford Nanopore Sequencing. J Open Source Software. 2019;4(34):1236.

[21] Wick RR, Judd LM, Gorrie CL, et al. Unicycler: resolving bacterial genome assemblies from short and long sequencing reads. PLoS Comput Biol. 2017;13(6):e1005595.

[22] Darling AE, Mau B, Perna NT. progressiveMauve: multiple genome alignment with gene gain, loss and rearrangement. PLoS One. 2010;5(6):e11147.

[23] Cingolani P, Platts A, Wang Le L, et al. A program for annotating and predicting the effects of single nucleotide polymorphisms, SnpEff: sNPs in the genome of Drosophila melanogaster strain w1118; iso-2; iso-3. Fly (Austin). 2012;6(2):80–92.

[24] Dedrick RM, Aull HG, Jacobs-Sera D, et al. The prophage and plasmid mobilome as a likely driver of Mycobacterium abscessus diversity. mBio. 2021;12(2). DOI:10.1128/mBio.03441-20

[25] Chawla Y, Upadhyay S, Khan S, et al. Protein kinase B (PknB) of Mycobacterium tuberculosis is essential for growth of the pathogen in vitro as well as for survival within the host. J Biol Chem. 2014;289(20):13858–13875.

[26] Zeng J, Platig J, Cheng TY, et al. Protein kinases PknA and PknB independently and coordinately regulate essential Mycobacterium tuberculosis physiologies and antimicrobial susceptibility. PLoS Pathog. 2020;16(4):e1008452.

[27] Giri A, Gupta S, Safi H, et al. Polymorphisms in Rv3806c (ubiA) and the upstream region of embA in relation to ethambutol resistance in clinical isolates of Mycobacterium tuberculosis from North India. Tuberculosis (Edinb). 2018;108:41–46.

[28] Li M-C, Chen R, Lin S-Q, et al. Detecting ethambutol resistance in Mycobacterium tuberculosis isolates in china: a comparison between phenotypic drug susceptibility testing methods and DNA sequencing of embAB. Front Microbiol. 2020;11:781.

[29] Korkegian A, Roberts DM, Blair R, Parish T: Mutations in the essential arabinosyltransferase EmbC lead to alterations in Mycobacterium tuberculosis lipoarabinomannan. J Biol Chem 2014, 289(51):35172–35181.

[30] Mendum TA, Chandran A, Williams K, et al. Transposon libraries identify novel Mycobacterium bovis BCG genes involved in the dynamic interactions required for BCG to persist during in vivo passage in cattle. BMC Genomics. 2019;20(1):431.

[31] Chen Y, Chen J, Zhang S, et al. Novel mutations associated with clofazimine resistance in Mycobacterium abscessus. Antimicrob Agents Chemother. 2018;62(7). DOI:10.1128/AAC.00544-18

[32] Bacon J, Dover LG, Hatch KA, et al. Lipid composition and transcriptional response of Mycobacterium tuberculosis grown under iron-limitation in continuous culture: identification of a novel wax ester. Microbiology. 2007;153(Pt 5):1435–1444.

[33] Parish T, Smith DA, Kendall S, et al. Deletion of two-component regulatory systems increases the virulence of Mycobacterium tuberculosis. Infect Immun. 2003;71(3):1134–1140.

[34] Gutierrez AV, Viljoen A, Ghigo E, et al. Glycopeptidolipids, a double-edged sword of the Mycobacterium abscessus complex. Front Microbiol. 2018;9:1145.

[35] Catherinot E, Clarissou J, Etienne G, et al. Hypervirulence of a rough variant of the Mycobacterium abscessus type strain. Infect Immun. 2007;75(2):1055–1058.

[36] Jones CM, Niederweis M. Role of porins in iron uptake by Mycobacterium smegmatis. J Bacteriol. 2010;192 (24):6411–6417.

[37] Goethe E, Laarmann K, Lührs J, et al. Critical Role of Zur and SmtB in Zinc Homeostasis of Mycobacterium smegmatis. mSystems. 2020;5(2). DOI:10.1128/mSystems.00880-19

[38] Sharbati-Tehrani S, Stephan J, Holland G, et al. Porins limit the intracellular persistence of Mycobacterium smegmatis. Microbiology. 2005;151(7):2403–2410.

[39] Danilchanka O, Pavlenok M, Niederweis M. Role of porins for uptake of antibiotics by Mycobacterium smegmatis. Antimicrob Agents Chemother. 2008;52(9):3127–3134.

[40] Li B, Guo Q, Mao Y, et al. Genetic evolution of Mycobacterium abscessus conferring clarithromycin resistance during long-term antibiotic therapy. Can Respir J. 2020;2020:7623828.

[41] Shea JE, Santangelo JD, Feldman RG. Signature-tagged mutagenesis in the identification of virulence genes in pathogens. Curr Opin Microbiol. 2000;3(5):451–458.

[42] Lucarelli D, Russo S, Garman E, et al. Crystal structure and function of the zinc uptake regulator FurB from Mycobacterium tuberculosis. J Biol Chem. 2007;282 (13):9914–9922.

[43] Umesiri FE, Sanki AK, Boucau J, et al. Recent advances toward the inhibition of mAG and LAM synthesis in Mycobacterium tuberculosis. Med Res Rev. 2010;30 (2):290–326.

[44] Richard M, Gutierrez AV, Viljoen A, et al. Mutations in the MAB_2299c TetR Regulator confer cross-resistance to clofazimine and bedaquiline in Mycobacterium abscessus. Antimicrob Agents Chemother. 2019;63(1). DOI:10.1128/AAC.01316-18

[45] Bailo R, Bhatt A, Ainsa JA. Lipid transport in Mycobacterium tuberculosis and its implications in virulence and drug development. Biochem Pharmacol. 2015;96 (3):159–167.

[46] Ryndak MB, Singh KK, Peng Z, et al. Transcriptional profile of Mycobacterium tuberculosis replicating in type II alveolar epithelial cells. PLoS One. 2015;10(4):e0123745.

[47] Dayaram YK, Talaue MT, Connell ND, et al. Characterization of a glutathione metabolic mutant of Mycobacterium tuberculosis and its resistance to glutathione and nitrosoglutathione. J Bacteriol. 2006;188(4):1364–1372.

[48] Pandey SD, Choudhury M, Yousuf S, et al. Iron-regulated protein HupB of Mycobacterium tuberculosis positively regulates siderophore biosynthesis and is essential for growth in macrophages. J Bacteriol. 2014;196(10):1853–1865.

[49] Brzostek A, Dziadek B, Rumijowska-Galewicz A, et al. Cholesterol oxidase is required for virulence of Mycobacterium tuberculosis. FEMS Microbiol Lett. 2007;275(1):106–112.

[50] Pawlik A, Garnier G, Orgeur M, et al. Identification and characterization of the genetic changes responsible for the characteristic smooth-to-rough morphotype alterations of clinically persistent Mycobacterium abscessus. Mol Microbiol. 2013;90(3):612–629.

[51] Pang L, Tian X, Pan W, et al. Structure and function of Mycobacterium glycopeptidolipids from comparative genomics perspective. J Cell Biochem. 2013;114 (8):1705–1713.

[52] Lipworth S, Hough N, Leach L, et al. Whole-Genome Sequencing for Predicting Clarithromycin Resistance in Mycobacterium abscessus. Antimicrob Agents Chemother. 2019;63:e01204-18.

[53] Ripoll F, Deshayes C, Pasek S, et al. Genomics of glyco-peptidolipid biosynthesis in Mycobacterium abscessus and M. chelonae. BMC Genomics. 2007;8(1):114.

[54] Davidson RM. A closer look at the genomic variation of geographically diverse Mycobacterium abscessus clones that cause human infection and disease. Front Microbiol. 2018;9:2988.

[55] Doyle RM, Rubio M, Dixon G, et al. Cross-transmission is not the source of new Mycobacterium abscessus infections in a multicenter cohort of cystic fibrosis patients. Clin Infect Dis. 2020;70(9):1855–1864.

[56] Wetzstein N, Kohl TA, Schultze TG, et al. Antimicrobial susceptibility and phylogenetic relations in a german cohort infected with Mycobacterium abscessus. J Clin Microbiol. 2020;58(12). DOI:10.1128/JCM.01813-20.

[57] Tortoli E, Kohl TA, Trovato A, et al. Mycobacterium abscessus in patients with cystic fibrosis: low impact of inter-human transmission in Italy. Eur Respir J. 2017;50(1):1602525.

[58] Schwarz C, Hogardt M. Empfehlungen an CF-Ambulanzen zur Risikominimierung einer möglichen Übertragung von-nicht-tuberkulösen Mykobakterien (z. B. Mycobacterium abscessus). Epidemiologisches Bulletin. 2014;13:107.

[59] Shoulah SA, Oschmann AM, Selim A, et al. Environmental Mycobacterium avium subsp. hominissuis have a higher probability to act as a recipient in conjugation than clinical strains. Plasmid. 2018;95:28–35.

[60] Rüger K, Hampel A, Billig S, et al. Characterization of rough and smooth morphotypes of Mycobacterium abscessus isolates from clinical specimens. J Clin Microbiol. 2014;52(1):244–250.

[61] Lavollay M, Dubée V, Heym B, et al. In vitro activity of cefoxitin and imipenem against Mycobacterium abscessus complex. Clin Microbiol Infect. 2014;20(5):O297–300.

[62] Wallace RJ Jr, Meier A, Brown BA, et al. Genetic basis for clarithromycin resistance among isolates of Mycobacterium chelonae and Mycobacterium abscessus. Antimicrob Agents Chemother. 1996;40(7):1676–1681.

[63] Smith DJ, Anderson GJ, Bell SC, et al. Elevated metal concentrations in the CF airway correlate with cellular injury and disease severity. J Cystic Fibrosis. 2014;13(3):289–295.

[64] Ranjan S, Yellaboina S, Ranjan A. IdeR in mycobacteria: from target recognition to physiological function. Crit Rev Microbiol. 2006;32(2):69–75.

[65] Fabrino DL, Bleck CK, Anes E, et al. Porins facilitate nitric oxide-mediated killing of mycobacteria. Microbes Infect. 2009;11(10–11):868–875.

[66] Ghazaei C. Mycobacterium tuberculosis and lipids: insights into molecular mechanisms from persistence to virulence. J Res Med Sci. 2018;23(1):63.

[67] Kreutzfeldt KM, McAdam PR, Claxton P, et al. Molecular longitudinal tracking of Mycobacterium abscessus spp. during chronic infection of the human lung. PLoS ONE. 2013;8(5):e63237.